

EFFICIENT TERNARY BLENDED HYBRID ORGANIC SOLAR CELLS: FULLERENE DERIVATIVE REPLACEMENT WITH METAL OXIDE NANOPARTICLES

M. IKRAM^{a*}, R. MURRAY^c, M. NAFEEES^a, M. IMRAN^d, S. ALI^a, S. ISMAT
SHAH^{b,c}

^a*Solar Application Lab, Department of Physics, G. C. University Lahore, 54000
Pakistan*

^b*Department of Materials Science and Engineering, University of Delaware,
Delaware, 19716, USA*

^c*Department of Physics and Astronomy, University of Delaware, Delaware,
19716 USA*

^d*Technical Institute of Physics and Chemistry, Chinese Academy of Sciences, 29
Zhongguancun East Road, Haidian District, Beijing 100190, People's Republic of
China*

In this study, we report the effects of mixing zinc oxide (ZnO) nanoparticles in the active layer on the performance of organic photovoltaics devices. The active layer primarily consists of various ratios of the organic electron donor poly(3-hexylthiophene (P3HT) and the electron acceptor [6,6] phenyl-C61-butyric acid methyl ester (PCBM) together with ZnO (less than 100 nm particle size) nanoparticles dissolved in xylene solvent. The weight ratio of PCBM to ZnO in the blend was varied, keeping the ratio of P3HT constant. The power conversion efficiency (PCE) improved by increasing the ZnO content in the active layer blend. The increase in PCE was mostly caused by the decrease in the series resistance (R_s) of the devices and increase in the open circuit voltage (V_{oc}) of the devices. The mixing also enhanced absorption in visible region and introduced red shift in the absorption spectra. The addition of ZnO increased the surface roughness of the active layer. The ZnO nanoparticles agglomerated as their ratio relative to PCBM and complete agglomeration was observed with no PCBM in the active layer blend.

(Received July 21, 2014; Accepted September 30, 2014)

Keywords: ZnO, Blend, Active layer, Series resistance, P3HT, PCE

1. Introduction

The world is facing an energy crisis and research is needed in this area using renewable energy resources. The conversion of the sun's rays into electricity is an environmental friendly and abundant energy source. The particular efficiency of silicon solar cells created from inorganic materials attained around 24% [1], working with expensive materials of high purity and energy intensive processing techniques. The alternative of silicon crystalline solar cell is 3rd generation solar cells; especially dye-sensitized solar cells (DSSC), conjugated polymer/fullerene bulk heterojunctions, small molecule thin films devices are attractive due to low cost, light-weight, portable, easy processing and flexible production [2]. New strategies of manufacturing solar cells that can scale up to significant sizes while remaining affordable are essential.

The bulk heterojunction (BHJ) structure is commonly used for organic solar cell (OSC) devices. This structure consists of an electron donor (polythiophene derivative) and an acceptor (fullerene) in an interpenetrating network blend. However, poor charge carrier mobility in most

* Corresponding author: mianraj.1981@gmail.com

conjugated polymers and quick recombination of photogenerated excitons (electron hole pair) limit the power conversion efficiency (PCE) of the solar cell.

This issue has been resolved by using inorganic semi-conductor nanostructures as electron acceptor in OSCs. These hybrid photovoltaics (PV) devices combine the exceptional properties of inorganic semiconductors such as high electron affinity, good stability and high electron mobility [3-4]. Therefore, organic-inorganic hybrid materials are potential candidates for use in PV cells [5]. The photoactive layer of a hybrid BHJ solar cell usually consists of physically blending inorganic semiconductor nanocrystals with conjugated polymers. However, the devices consisting of the hybrid material blends often encounter problems, including poor compatibility [6], thus decreasing the interfacial area between inorganic semiconductor and conjugated polymers and limiting the efficiency of the resulting devices. Different methods have been applied to manage these issues, such as the surface modification of nanocrystals, in-situ fabrication methods, the use of co-solvent mixtures, etc. [7-13].

In this work, we mixed ZnO (≤ 100 nm) nanoparticles in P3HT:PCBM blend to fabricate ternary material based hybrid solar cells [14]. Our work aims to study the effects of ZnO nanoparticles on optical, morphological and electrical properties of the active layer blend and hence on PCE of the devices. The addition of ZnO nanoparticles increased PCE of the devices in the presence of PCBM only.

2. Experimental Details

The glass substrates pre-coated with indium tin oxide (ITO) of Delta Technologies USA, with sheet resistance of 8-12 Ω/\square were used for the device fabrication. Conducting polymer (poly(3,4- ethylene dioxythiophene)-polystyrenesulfonate) (PEDOT:PSS) was obtained from Heraeus Material Technology LLC, USA. Highly regioregular P3HT (P200), ZnO nanoparticles and PCBM were purchased from Rieke Metal, Sigma Aldrich and Nano-C USA, respectively. All materials were used as received without further purification.

The hybrid solar cells were prepared with different weight compositions of PCBM, ZnO and P3HT in the active layer of the devices. Hybrid solar cell devices were fabricated by spin coating PEDOT:PSS at 3000 rpm for 60 s on ultrasonically cleaned ITO glass substrates. The samples were baked in N₂ environment inside glovebox at 130°C for 10 minutes. The blends of P3HT:PCBM:ZnO of various weight ratios (1:0.7:0, 1:0.55:0.15, 1:0.35:0.35, 1:0.15:0.55 and 1:0:0.7) in 1ml xylene solvent after stirring 12 h at 40°C were spun on the top of PEDOT:PSS layer. The spun films were annealed on the hotplate at 150°C for 15 minutes in nitrogen environment. Upon an active layer a thin layer of LiF (0.3 nm) and aluminum (100 nm) were evaporated under high vacuum with an active area of 0.4 cm². The device structure was Al/LiF/P3HT:PCBM:ZnO/PEDOT:PSS/ITO as shown in fig 1.

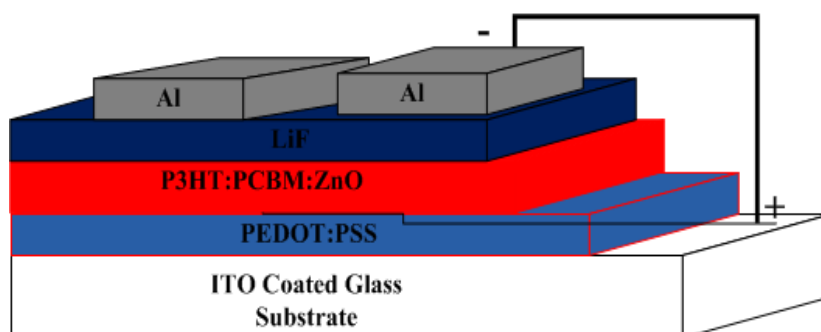


Fig. 1. Schematic diagram of hybrid solar cells

3. Results and discussion

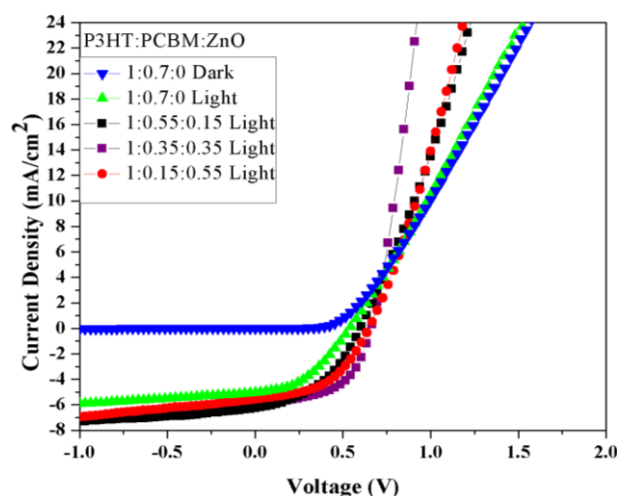


Fig.2. J-V characteristics of different ratios of P3HT:PCBM:ZnO devices

The current density vs voltage (J-V) curves obtained under dark and light conditions of 100 mWcm^{-2} are shown in Fig. 2. Figure 2 shows that the incorporation of ZnO nanoparticles in the active layer decreased R_s and hence increased FF of the devices. Various ratios of the blends were used in the active layer and results are summarized in Table 1.

The table indicates that mixing of ZnO in the active layer of the devices, while maintaining the amount of acceptor material, increases PCE from $1.13 \pm 0.1\%$ to $2.14 \pm 0.2\%$. The table shows that R_s decreased from $39 \text{ } \Omega\text{-cm}^2$ to $17 \text{ } \Omega\text{-cm}^2$, with addition of ZnO, in the presence of PCBM in the active layer. The decrease in R_s is attributed to decrease in bulk resistivity with the addition of ZnO, as the addition improves percolation network of the active layer [14]. The increase in R_{sh} (Table-1) is attributed to suppression of leakage current due to ZnO nanoparticles network [15,16].

Table 1: Device parameters obtained from J-V curves in Fig. 2

P3HT:PCBM:ZnO	V_{oc} (V)	J_{sc} (mA/cm^2)	FF (%)	R_{sh} ($\Omega\text{-cm}^2$)	R_s ($\Omega\text{-cm}^2$)	PCE (%)
1:0.7:0	0.538	5.03	41.74	664	39	1.13 ± 0.1
1:0.55:0.15	0.602	6.33	42.85	480	19	1.62 ± 0.3
1:0.35:0.35	0.661	6.07	54.19	672	16	2.14 ± 0.2
1:0.15:0.55	0.648	5.64	48.18	632	17	1.74 ± 0.1
1:0:0.7	0.475	0.01	34.14	78400	51	0.001

The energy level diagram of the devices are shown in Fig. 3 [17]. Excitons are created at the interface of P3HT and PCBM. In our case the holes transfer towards ITO electrode after passing through hole transport layer (PEDOT:PSS), and electrons are transported to the cathode due to higher electron mobility and lower conduction band of ZnO nanoparticles.

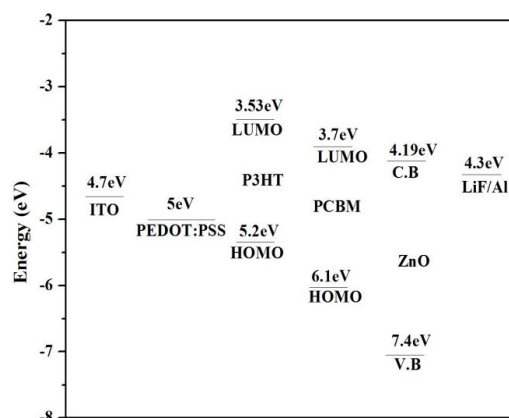


Fig. 3: Energy level diagram with incorporation of ZnO nanoparticles in hybrid solar cells

The observed decrease in R_s and increase in R_{sh} reduced the leakage current and led to significant increase in FF and V_{oc} of the devices with increasing amount of ZnO nanoparticles in the active layer [18,19]. The increase observed in J_{sc} and FF is attributed to percolation network of ZnO nanoparticles that facilitates the electron transport in the photoactive layer and an electric field is formed between heterojunction of organic material and ZnO nanoparticles [17,20]. The low efficiency of the device with ratio 1:0:0.7 is attributed to agglomeration of ZnO nanoparticles. The excess amount of ZnO in the active layer of P3HT blend broke the BHJ network due to agglomeration and device stopped generating current that led to the poor solar cell performances.

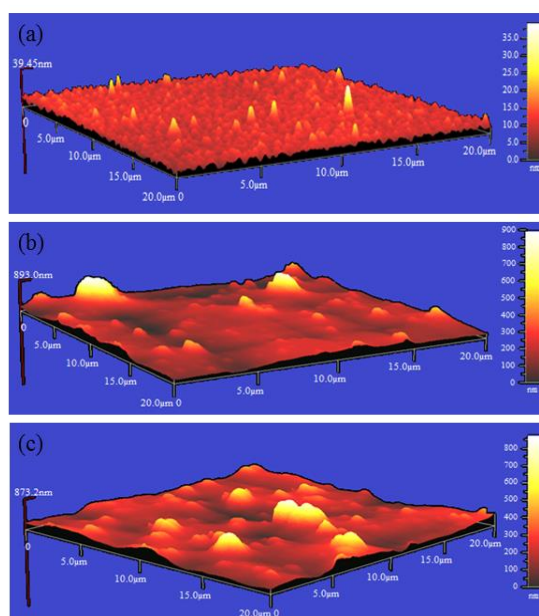


Fig. 4. AFM images of P3HT:PCBM:ZnO with ratio 1:0.7:0 (a) 1:0.35:0.35 (b) and 1:0.15:0.55 (c)

Fig. 4(a)-4(c) represent images of different ratios (1:0.7:0, 1:0.35:0.35, 1:0.15:0.55) of P3HT:PCBM:ZnO active layers obtained using atomic force microscope (AFM). Figure 4a displays the surface is rough with a few needle type feature with RMS roughness value of 5.7 nm. Figure 3b and 3c indicate the formation of small and large agglomerations on the surface with RMS roughness of 9.7 nm and 26.4 nm respectively. The mixing of ZnO nanoparticles in the active layer of P3HT:PCBM enhanced the surface roughness of the film.

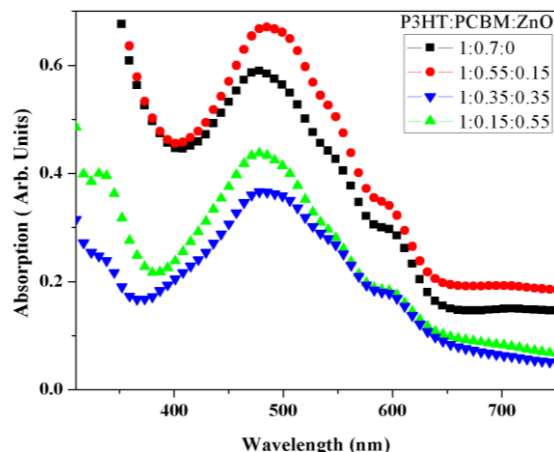


Fig. 5. Absorption spectra of different ratios of P3HT:PCBM:ZnO devices

Fig. 5 shows that absorption spectra of binary system P3HT:PCBM and ternary system of P3HT:PCBM:ZnO active layers. The absorption increased with the incorporation of ZnO in the blend of P3HT:PCBM and introduced red shift. The observed red shift was manifested to improve the crystallinity of P3HT. This improvement in crystallinity of P3HT is obvious from the more pronounced absorption shoulder witnessed around 600 nm [21,22] in Figure 5. As discussed earlier, roughness increased in the presence of ZnO nanoparticles in the active layer. The surface with high roughness might reflect more light in the active layer. This leads to slightly increased absorption with optimum amount of ZnO mixed in the blend of active layer [17].

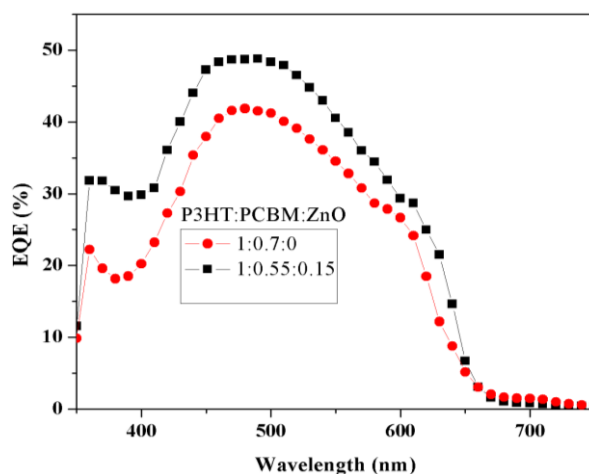


Fig.6. EQE curves of different ratios of P3HT:PCBM:ZnO based devices

The EQE curves of various ratios of P3HT:PCBM:ZnO are shown in Fig.6. The figure shows the improved EQE with addition of ZnO in active layer of the devices. This improve in EQE over the wavelength 375-650 nm contributes to the increase in PCE of the devices. The enhancement in EQE is attributed to an increase absorption in the active layer and increased in the charge carrier mobility with incorporation of ZnO nanoparticles [23].

4. Conclusions

Effect of incorporation of ZnO nanoparticles in active layer of P3HT:PCBM solar cells is studied using xylene as the solvent. The mixing shows increase in PCE of the device from

1.13±0.1 % to 2.14±0.2 %. The PCE improved most probably due to decrease in R_s of the devices. The Voc, Jsc, FF, EQE and absorption of the devices increase with increasing amount of ZnO nanoparticles in the active layer blend of P3HT:PCBM. The ZnO nanoparticles form small and large aggregations with increasing amount of ZnO in the active layer and enhanced the surface roughness. The PCBM also acts as a surfactant material in the active layer blend and ZnO nanoparticles completely agglomerate in the absence of fullerene derivative in the active layer blend.

Acknowledgement

The work is jointly supported by National Academy of Science (NAS), USA and Higher Education Commission (HEC) Pakistan under the grant # PGA-P210859.

References

- [1] M. Green, *Progr. Photovolt* **9**, 123, (2001).
- [2] K. Walzer, B. Maennig, M. Pfeiffer, K. Leo, *Chem. Rev* **107**, 1233(2007).
- [3] J. Boucle, S. Chyla, M.S.P. Shaffer, J.R. Durrant, D.D.C. Bradley, J. Nelson, *Advanced Functional Materials* **18**, 622 (2008).
- [4] A.M. Smith, S. Nie, *Accounts of Chemical Research* **43**, 190 (2010).
- [5] J.C.Liu, W.L. Wang, H.Z. Yu, Z. L. Wu, J.B. Peng, Y. Cao, *Solar Energy Materials and Solar Cells* **92**, 1403 (2008).
- [6] Z.Q. Lin, *Chemistry A European Journal* **14**, 6294 (2008).
- [7] W.U. Huynh, J.J. Dittmer, A.P. Alivisatos, *Hybrid Nanorod-Polymer Solar Cells*, *Science* **295**, 2425 (2002).
- [8] W.J.E. Beek, M.M. Wienk, M. Kemerink, X.N. Yang, R.A.J. Janssen, *Journal of Physical Chemistry B* **109**, 9505 (2005).
- [9] S. Dayal, N. Kopidakis, D.C. Olson, D.S. Ginley, G. Rumbles, *Journal of the American Chemical Society* **131**, 17726 (2009).
- [10] W.J.E. Beek, L.H. Slooff, M.M. Wienk, J.M. Kroon, R.A.J. Janssen, *Advanced Functional Materials* **15**, 1703 (2005).
- [11] X.M. Peng, L.Zhang, Y.W. Chen, F.Li, W.H. Zhou, *Applied Surface Science* **256**, 2948 (2010).
- [12] H.W. Geng, Y. Guo, R.X. Peng, S. K. Han, M.T. Wang, *Solar Energy Materials and Solar Cells* **94**, 1293, (2010).
- [13] P. Atienzar, T. Ishwara, M. Horie, J.R. Durrant, J. Nelson, *Journal of Materials Chemistry* **19**, 5377 (2009).
- [14] J. F. Lin, G. Y. Tu, C. C. Ho, C. Y. Chang, W. C. Yei, H. S. Hsu, Y. F. Chen, W. F. Su, *ACS Appl Mater Interfaces* **5**, 1009 (2013).
- [15] B. R. Saunders, M. L. Turner, *Adv. Colloid Interface* **1**, 138 (2008).
- [16] J. S. Huang, C. Y. Chou, M. Y. Liu, K. H. Tsai, W. H. Lin, C. F. Lin, *Org. Electron* **10**, 1060(2009).
- [17] S. H. Oh, S. J. Heo, J. S. Yang, H. J. Kim, *Appl. Mater. Interfaces* **5**, 11530 (2013).
- [18] T. P. Osedach, L. Y. Chang, S. M. Geyer, D. Wanger, M. T. Binda, A. C. Arango, M. G. Bawendi, V. Bulovic, *ACS Nano* **4**, 3743 (2010).
- [19] E. L. Lim, C. C. Yap, M. Yahaya, M. M. Salleh, *Journal of Physics* **431**, 012017(2013).
- [20] H. Fu, M. Choi, W. Luan, Y. S. Kim, S. T. Tu, *Solid-State Electronics* **69**, 50 (2012).
- [21] M. Ikram, R. Murray, A. Hussain, S. Ali, S. Ismat Shah, *Mater. Sci. Eng. B* **189**, 64 (2014).
- [22] L. Zeng, C. W. Tang, S. H. Chen, *Appl. Phys. Lett.* **97**: 053305 (2010).
- [23] G. Li, V. Shrotriya, Y. Yao, J. Huang, Y. Yang, *J. Mater. Chem* **17**, 3126 (2007).